Green's function studies of phonon transport across Si/Ge superlattices

Zhiting Tian, Keivan Esfarjani, and Gang Chen*

Department of Mechanical Engineering, Massachusetts Institute of Technology, Cambridge, Massachusetts 02139, USA

(Received 12 March 2014; revised manuscript received 7 May 2014; published 10 June 2014)

Understanding and manipulating coherent phonon transport in solids is of interest both for enhancing the fundamental understanding of thermal transport as well as for many practical applications, including thermoelectrics. In this study, we investigate phonon transmission across Si/Ge superlattices using the Green's function method with first-principles force constants derived from *ab initio* density functional theory. By keeping the period thickness fixed while changing the number of periods, we show that interface roughness partially destroys coherent phonon transport, especially at high temperatures. The competition between the low-frequency coherent modes and high-frequency incoherent modes leads to an optimum period length for minimum thermal conductivity. To destroy coherence of the low-frequency modes, scattering length scale on the order of period length is required. This finding is useful to guide the design of superlattices to reach even lower thermal conductivity.

DOI: 10.1103/PhysRevB.89.235307 PACS number(s): 63.20.dk, 68.35.Ct, 63.22.Np

I. INTRODUCTION

Thermal properties of semiconductor superlattices have been under intense investigation due to their potential uses in thermoelectric energy conversion [1–3] and optoelectronic devices [4]. The thermal conductivity of superlattices can be even lower than their alloy counterparts [5–8]. Although diffuse scattering at interfaces is responsible for the remarkable thermal conductivity reduction [9,10], coherent phonon transport has been experimentally observed in GaAs/AlAs superlattices [11] and perovskite oxides [12]. To further reduce the thermal conductivity for thermoelectric applications, it is crucial to understand and control the different phonon transport modes in superlattices.

Phonon heat conduction in superlattices can be attributed to incoherent and coherent phonon modes. Coherent modes preserve their phase as they propagate through multiple interfaces. For these phonons, Bloch mode extends through the whole structure, and the superlattices can be treated as a homogeneous material with its own unit cell and phonon dispersion. If, due to roughness or other structures, interfaces destroy the constructive interference of waves, phonon modes lose their phase information and their transport becomes incoherent. For these modes, superlattices act as a composite made of a stack of two alternating materials, each having their own phonon dispersion.

Previous theoretical studies on superlattices have focused on changing periodicity. Most common theories developed to understand phonon transport in superlattices fall into one of two pictures: the incoherent particle picture, which is rooted in solving the Boltzmann transport equation [9,13], and the coherent wave picture, where lattice dynamics calculations are employed [14–16]. Either picture could fully explain the experimentally observed thermal conductivity trend as a function of period length in both in-plane and cross-plane directions, though [3]. A combination of both pictures is desired. Lattice dynamics based on damped wave functions was used to predict a minimum in the thermal conductivity of superlattices in the cross-plane direction [17,18]. More recently, a perturbation method based on the Fermi golden rule [11,19,20] was developed, but the method may have limitations on treating interface scattering, as strong scattering may not be captured by perturbation. One alternative approach is to use molecular dynamics simulations [21,22], which do not assume the nature of phonon transport but are classical in nature. Yet the empirical potentials involved in molecular dynamics limit accuracy, and it is difficult to explore the detailed phonon mode behavior.

The green's function method has been applied to study phonon transport across single and multiple Si/Ge interfaces. For single Si/Ge interfaces, effects of strain [23], lattice mismatch [24], and interface roughness [25,26] on phonon transmission have been investigated. Green's function study on Si/Ge superlattices, however, is scarce. Zhang *et al.* [23] briefly discussed the effect of number of interfaces on the overall thermal resistance across multiple Si/Ge interfaces, while transmission function was not detailed. In this study, we use the Green's function method to investigate coherent phonon transport across Si/Ge superlattices. First-principles force constants have been incorporated as in our previous work on single Si/Ge interfaces [25]. We calculate the phonon transmission and corresponding thermal conductivity of Si/Ge superlattices with varying interface roughnesses. Inspired by recent experiments [11], we keep the period thickness of the superlattices fixed while changing the number of periods. We observe coherent phonon transport in smooth-interfaced superlattices, and partially coherent and partially incoherent transport in rough-interfaced superlattices. While the low-frequency modes maintain their coherence in both cases, roughness is able to destroy the coherence of the higher frequency modes. To destroy the coherence of low-frequency modes, a scattering length scale comparable to period length is needed. These fundamental observations are crucial for the intelligent control of coherent vs incoherent transport in superlattices.

II. METHODOLOGY

We follow the same atomistic Green's function method [23,27] we applied for a single Si/Ge interface [25]. The only

*Corresponding author: gchen2@mit.edu

FIG. 1. (Color online) Schematic of the system setup: the left reservoir is pure Si, the right reservoir is pure Ge, the center region is the Si/Ge superlattices.

difference is that, in this study, we use Si/Ge superlattices as the center region, as shown in Fig. 1. As a brief overview, we employ the force constant ϕ_C from *ab initio* density functional theory into the Green's function to determine the transmission function. The retarded Green's function is given by

$$G^R(\omega) = [\omega^2 I - \phi_C - \Sigma_L(\omega) - \Sigma_R(\omega)]^{-1}, \quad (1)$$

where G^R is the retarded Green's function, ω is the phonon frequency, ϕ_C represents the onsite force constants of the center region, and the self-energy Σ_α describes the effect of the lead α on the center block. The transmission function $\Xi(\omega)$ is given as a trace over the Green's function of the center region and the coupling terms between the leads and the center

$$\Xi(\omega) = Tr[\Gamma_L(\omega)G^R(\omega)\Gamma_R(\omega)G^A(\omega)], \quad (2)$$

where $\Gamma_\alpha = i[\Sigma_\alpha^R - \Sigma_\alpha^A]$ describes the rate at which phonons enter and exit the leads. In these calculations, transverse periodic boundary conditions are assumed, and the above formulas hold for every single transverse momentum, over which a final summation needs to be performed in order to obtain the total transmission.

The interface transmittance is then defined as

$$\tau(\omega) = \frac{\Xi(\omega)}{\Xi_{\text{pure}}(\omega)}. \quad (3)$$

In our system setup, we use $\Xi_{\text{pure}}(\omega) = \Xi_{Si}(\omega)$.

The two-probe thermal conductance per unit area σ based on the total transmission function $\Xi(\omega)$ is calculated using the Landauer formula [28]

$$\sigma(T) = \frac{1}{S} \times \frac{1}{2\pi} \int_0^\infty \hbar\omega \frac{\partial f(\omega,T)}{\partial T} \Xi(\omega) d\omega, \quad (4a)$$

where f is the Bose-Einstein distribution and s is the cross-sectional area of the simulation cell perpendicular to the direction of heat flow. The four-probe conductance can then be written [25]

$$\sigma'(T) = \sigma(T) \times \frac{1}{1 - \frac{1}{2}\left(\frac{\sigma(T)}{\sigma_1(T)} + \frac{\sigma(T)}{\sigma_2(T)}\right)}. \quad (4b)$$

Although the difference in thermal conductance between the two-probe and four-probe formulas becomes small as the number of interfaces increases, we use the four-probe formula throughout this study to be consistent with our previous calculation of single-interface and experiments.

The thermal conductivity of a sample length L is defined to be L times the four-probe conductance:

$$k = \sigma' L. \quad (5)$$

The calculations in this paper do not include phonon-phonon scattering. According to experimental [5,6] and modeling [9,19,21] results on Si/Ge superlattices, anharmonic effects are not important for temperatures below 500 K. The anharmonicity would become important when the phonon mean free path due to anharmonicity becomes smaller than the superlattice length L. In the harmonic regime, specular scattering leads to coherent wave effects [29–31], while diffuse scattering could destroy coherence.

III. RESULTS AND DISCUSSION

For incoherent transport, the interfaces behave like a series of thermal resistors, and the effective thermal conductivity becomes independent of the number of periods. For coherent transport, thermal resistance keeps constant with respect to number of periods, and thermal conductivity increases linearly with increasing number of periods. The thermal conductivities for smooth- and rough-interfaced superlattices are shown in Fig. 2(a). The thermal conductivity of smooth-interfaced superlattices demonstrates a linear increase with respect to the number of periods, indicating coherent transport at 300 K, although ultimately anharmonicity limits the number of periods over which transport is coherent. The thermal conductivity of rough-interfaced superlattices increases more slowly than linear, indicating partially coherent and partially incoherent transport. Another noticeable point is that roughness increases the thermal conductivity of small-period superlattices, contrary to conventional wisdom. This is because atomic roughness generates smoother change of density of states between layers [25]. Note that competition between better transition of the vibrational spectrum and diffuse scattering, both introduced by atomic mixing, gives rise to the enhancement of phonon transmission at small thicknesses of roughness ($\sim$1 nm for Si/Ge case) and small number of periods. This conclusion does not conflict with experimentally observed lower thermal conductivity caused by atomic mixing at larger length scales [32].

We then compare transmittance across smooth-interfaced superlattices [Fig. 2(b)] with that of rough-interfaced ones [Fig. 2(c)]. When the number of periods equals 1, it reverts to the single Si/Ge interface we investigated before [25], which we include as a reference. What we are mainly interested in here are multiple interfaces. For number of periods >1, there are clearly two frequency regimes: the low-frequency regime and the higher frequency regime separated by vertical lines at 55.6 cm^{-1}. The low-frequency regime is defined as the region where transmittance does not change as the number of periods is increased. This indicates that low-frequency, long-wavelength phonons pass through the entirety of the superlattices as if it is a homogeneous medium. They form passing bands and transport coherently. The low-frequency regime is the same for both smooth and rough superlattices. In the rough case, the constancy of transmittance vs the number of periods for low-frequency phonons is due to the fact that such phonons have wavelengths larger than the roughness scale and thus see an effectively homogeneous interface of atoms with mass intermediate between Si and Ge. As such, they do not get scattered by roughness at the interface; thus, similar to ideal interfaces, their transmittance does not change with the number of periods. In the higher frequency regime, the transmittance for smooth-interfaced superlattices no longer changes as the number of periods becomes larger than five, suggesting the formation of minibands. Because

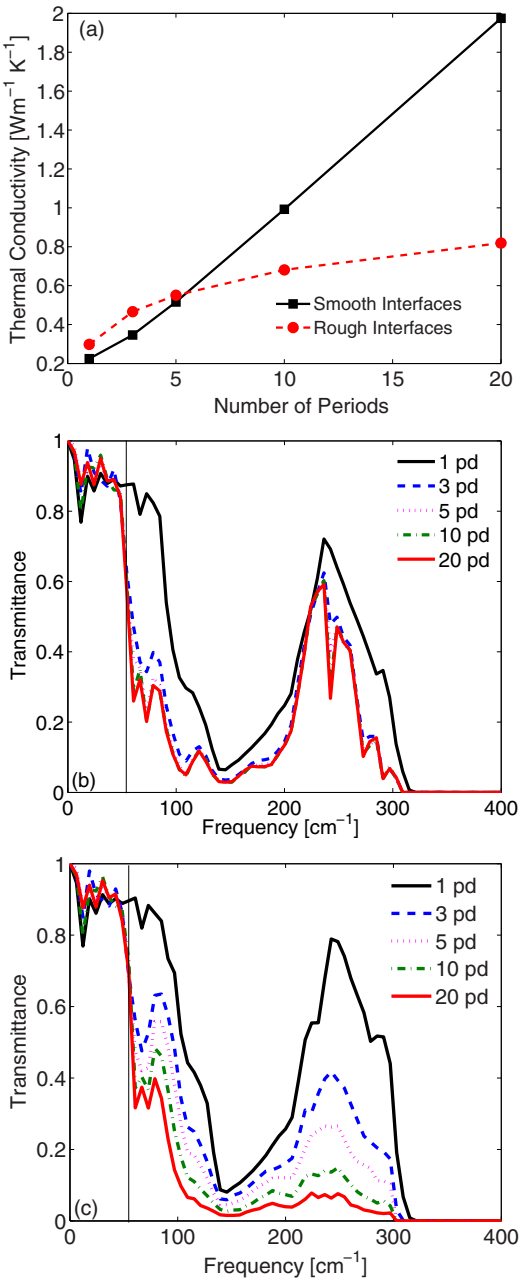

FIG. 2. (Color online) (a) Thermal conductivity of superlattices as a function of number of periods for smooth and rough superlattices at $T = 300$ K. (b) Transmittance as a function of frequency for superlattices (period = 2a) with smooth interfaces; (c) Transmittance as a function of frequency for superlattices (period = 2a) with rough interfaces.

the superlattice eigenstates are formed from the constructive interference between all multiple reflected waves, the wave needs to go a few periods away and be reflected back a few times in order to get a coherent eigenstate of the superlattice. In contrast, the transmittance for rough-interfaced superlattices keeps dropping due to more diffuse scattering at the interfaces. In other words, roughness destroys coherence of higher frequency modes.

To unveil the cutoff frequency ω_{cutoff} of the low-frequency regime, we plot the phonon dispersion of SiGe superlattice

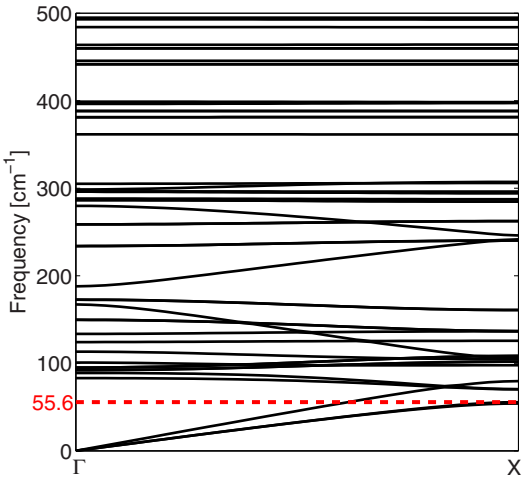

FIG. 3. (Color online) Phonon dispersion of Si/Ge superlattice with period $l = 2a$ in [100] direction.

with period length $l = 2a$ in the [100] direction [Fig. 3]. The zone boundary frequency of the lowest acoustic branch is 55.6 cm^{-1}. It is intriguing that the cutoff frequency is the lowest acoustic phonon branch at the folded Brillouin zone edge. Although some of the higher frequency phonons have a long wavelength in the folded zone representation, they are unable to maintain their coherence. Therefore, phonon wavelengths of higher frequency modes in the folded zone do not matter. We expect that this argument generally holds for different materials. As the period length increases, the first Brillouin zone becomes shorter because the edge of the folded zone is proportional to the inverse of the period length. Thus, the cutoff frequency of the totally coherent regime is determined by the reduced first Brillouin zone, or the period length. It is, therefore, difficult to destroy the coherence of the low-frequency modes unless a scattering length scale comparable to the period length can be introduced.

We then explore the temperature dependence of coherent and incoherent phonon transport. This temperature dependence comes only from phonon occupation or heat capacity. At all temperatures, phonons with frequencies smaller than the cutoff frequency yield a linearly increasing thermal conductivity as a function of number of periods, as shown in Fig. 4(a)–4(c). To illustrate this effect, we choose temperatures of 20, 50, and 300 K, which correspond to frequencies of 13.9, 34.7, and 208.1 cm^{-1} respectively. These are to be compared with the cutoff frequency of 55.6 cm^{-1}. At low temperatures, only low-frequency modes are excited; thus, the phonon transport is mostly coherent. As the temperature increases, more and more high-frequency modes are excited, and incoherent phonon transport plays a more and more important role. Correspondingly, we observe that thermal conductivity increases more slowly than linear and becomes flatter as the number of periods increases.

In our previous paper on single Si/Ge interfaces [25], we found that the conductance at a single Si/Ge interface is an order of magnitude lower than the extracted experimental thermal conductance from Si/Ge superlattices, assuming thermal resistance only happens at the interfaces. We predicted that the

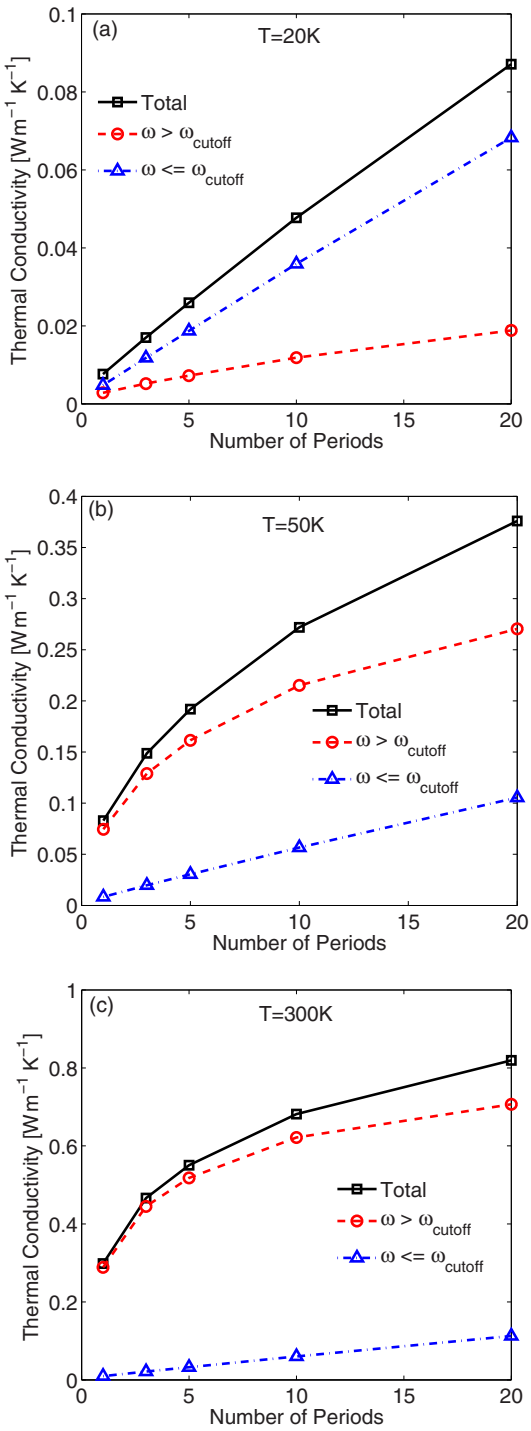

FIG. 4. (Color online) Total thermal conductivity and contribution from phonons with frequencies larger than the cutoff frequency and not larger than the cutoff frequency at (a) $T = 20$ K, (b) 50 K, and (c) 300 K.

discrepancy comes from the long-wavelength phonons, which maintain their coherence. Now with coherent transport, the calculated thermal conductance per interface increases with the number of periods and matches well with experiments (Fig. 5). Although the size of the superlattices is much smaller than that of the experimental samples [6,33] due to

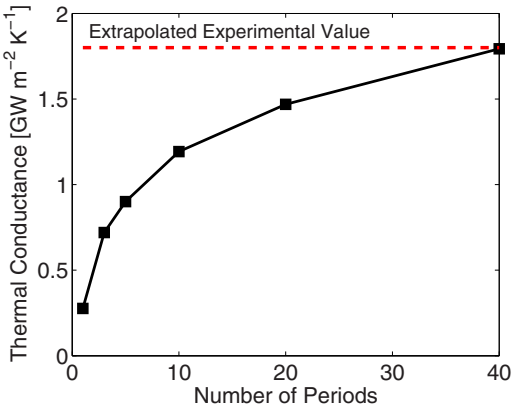

FIG. 5. (Color online) Normalized thermal conductance per interface as a function of number of periods for rough-interfaced superlattices with period length $l = 2a$. The experimental value is extrapolated from the sample of period length $l = 4.4$ nm and 100 periods [6].

computational limitations, we can at least see that the trend is consistent. It states that thermal conductance is not intrinsic to the interface but depends on what exists on both sides of the interface.

To destroy coherence in rough superlattices for the purpose of reducing thermal conductivity, there are two competing effects as the period length increases: (1) the low-frequency regime with totally coherent transport shrinks, which is beneficial, and (2) the interface density decreases and the importance of interface roughness decreases, which is detrimental. We plot thermal conductivity as a function of superlattice length for period length $l = a, 2a$, and $4a$, respectively in Fig. 6. At the same superlattice length, superlattices with period length $l = 2a = 1nm$ possess minimum thermal conductivity. The crossover from a coherent to incoherent regime is naturally included in our formulation. We thus observe the minimum thermal conductivity of superlattices [12,18,20] under the atomistic Green's function framework.

We then introduce a simple model in Eq. (6) to identify the dependence of thermal conductivity on period length. We

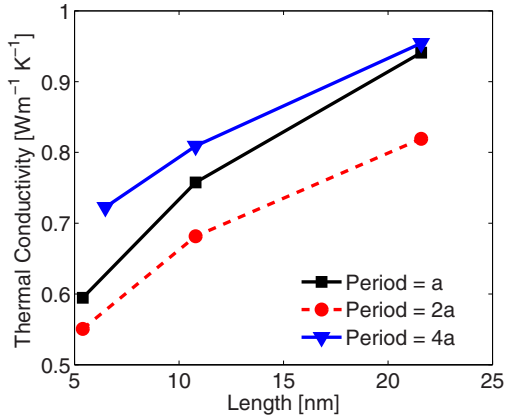

FIG. 6. (Color online) Thermal conductivity of rough-interfaced superlattices as a function of superlattice length for period length $l = a, 2a$, and $4a$ at 300 K.

write the thermal conductivity as a sum over the contribution of acoustic (the three low-lying folded acoustic phonons) and optical (rest of the bands) phonons

$$\begin{aligned} k &= k_{ac} + k_{op} \\ &= \int_0^{\omega_{\text{cutoff}}} C_v(\omega) D(\omega) v(\omega) \Lambda(\omega) d\omega \\ &\quad + \int_{\omega_{\text{cutoff}}}^{\omega_{\max}} C_v(\omega) D(\omega) v(\omega) \Lambda(\omega) d\omega \end{aligned} \tag{6}$$

where $\omega_{\max}$ represents the highest phonon frequency. For acoustic phonons, we assume specific heat $C_v(\omega) = k_B$, density of states $D(\omega) = A\omega^2$ (A is a coefficient that can be determined from the Debye approximation or lattice dynamics calculations), $v(\omega) = c$ (average speed of sound of acoustic modes), and $\Lambda(\omega) = L$ (in the absence of anharmonicity, and for short enough samples, we assume that acoustic phonon scattering occurs at the sample boundaries). Then

$$k_{ac} = \int_0^{\omega_{\text{cutoff}}} A\omega^2 k_B c L d\omega = \frac{3}{l A_{\text{trans}}} k_B c L \tag{7}$$

since $\int_0^{\omega_{\text{cutoff}}} A\omega^2 d\omega = \frac{3}{\Omega_{\text{cell}}}$ and $\Omega_{\text{cell}} = l A_{\text{trans}}$ with A_{trans} being the area of the unit cell in the transverse direction. For optical phonons, we use $C_v(\omega) = \hbar\omega \frac{\partial f}{\partial T}$, $D(\omega) = \bar{D}$ (average density of states in a given volume per unit frequency interval), $v(\omega) = c_{op}$(average speed of sound for optical modes, which is much smaller than speed of sound), and $\Lambda(\omega) = \frac{1}{2}\frac{1+p}{1-p} l$, where p accounts for the probability of pure specular scattering at each interface, and we have assumed the thickness of each medium to be equal to half the superlattice period

$$\begin{aligned} k_{op} &= \int_{\omega_{\text{cutoff}}}^{\omega_{\max}} \hbar\omega \frac{\partial f}{\partial T} \bar{D} c_{op} \frac{1}{2} \frac{1+p}{1-p} l d\omega \\ &\approx \frac{3N-3}{\Omega_{\text{cell}}} k_B c_{op} \frac{1}{2} \frac{1+p}{1-p} l \end{aligned} \tag{8}$$

if further assumption of $\frac{\hbar\omega}{k_B T} \ll 1$ is made. Here N is the total number of atoms in a period. Therefore, the overall conductivity (neglecting anharmonicity) would be a sum of

$$k = \frac{3}{l A_{\text{trans}}} k_B c \mathrm{L} + \frac{3N-3}{\Omega_{\text{cell}}} k_B c_{op} \frac{1}{2} \frac{1+p}{1-p} l. \tag{9}$$

Equation (9) has a minimum at an optimum period length at

$$l_{\text{opt}} = \sqrt{\frac{3\Omega_{\text{cell}} c \mathrm{L}(1-p)}{(3N-3) A_{\text{trans}} c_{op}(1+p)}} \approx \sqrt{\frac{\Omega_{\text{cell0}} c \mathrm{L}(1-p)}{N_0 A_{\text{trans}} c_{op}(1+p)}}, \tag{10}$$

where Ω_{cell0} and N_0 are the volume and number of atoms in a unit cell, respectively. It is noteworthy that the optimum period length depends on superlattice length, because the relative contribution from coherent and incoherent phonons would vary as the superlattice lengths change. When designing superlattices to reduce thermal conductivity, the optimum period length would be desirable. For the SiGe superlattices considered in this work, $N_0 = 8, \Omega_{\text{cell0}} = a^3$, $A_{\text{trans}} = 3a \times 3a$, and $a = 0.54$ nm. We assume $c = 5400$ m/s(speed of sound for germanium), $c_{op} = 100$ m/s, and $p = 0.5$. This leads to $l_{\text{opt}} = 0.82$ nm at $L = 5$ nm, $l_{\text{opt}} = 1.16$ nm at $L = 10$ nm, and $l_{\text{opt}} = 1.64$ nm at $L = 20$ nm. All the optimum period lengths are close to $2a = 1.08$ nm, which is consistent with our calculations using the atomistic Green's function method. In strongly anharmonic materials, however, k_{op} would be independent of l, and there is no minimum thermal conductivity.

IV. CONCLUSION

We apply the atomistic Green's function method to calculate phonon transmission across Si/Ge superlattices. We focus our discussion on coherent vs incoherent phonon transport in superlattices. We show totally coherent phonon transport in smooth-interfaced superlattices and partially coherent and partially incoherent phonon transport in rough-interfaced superlattices. We demonstrate that the contribution from coherent phonons decreases in rough-interfaced superlattices as temperature increases. To obtain the lowest thermal conductivity, there is an optimum length resulting from the competition between coherence of low-frequency phonons and incoherence of high-frequency phonons caused by interface scattering when anharmonicity is negligible. Our theoretical study complements earlier experiments, providing guidance for the design of superlattices.

ACKNOWLEDGMENTS

We acknowledge discussions with Bo Qiu and Maria N. Luckyanova. This material is supported by the S3TEC, an Energy Frontier Research Center funded by the U.S. Department of Energy, Office of Science, Office of Basic Energy Sciences under Award No. DE-FG02-09ER46577.

[1] G. Chen, M. S. Dresselhaus, G. Dresselhaus, J. P. Fleurial, and T. Caillat, International Materials Reviews **48**, 45 (2003).
[2] M. S. Dresselhaus, G. Chen, M. Y. Tang, R. G. Yang, H. Lee, D. Z. Wang, Z. F. Ren, J. P. Fleurial, and P. Gogna, Adv. Mater. **19**, 1043 (2007).
[3] Z. T. Tian, S. Lee, and G. Chen, J. Heat Transfer **135**, 061605 (2013).
[4] C. L. Tien and G. Chen, J. Heat Transfer **116**, 799 (1994).
[5] S. M. Lee, D. G. Cahill, and R. Venkatasubramanian, Appl. Phys. Lett. **70**, 2957 (1997).
[6] T. Borca-Tasciuc, W. L. Liu, J. L. Liu, T. F. Zeng, D. W. Song, C. D. Moore, G. Chen, K. L. Wang, M. S. Goorsky, T. Radetic, R. Gronsky, T. Koga, and M. S. Dresselhaus, Superlattices Microstruct. **28**, 199 (2000).

[7] W. S. Capinski, H. J. Maris, T. Ruf, M. Cardona, K. Ploog, and D. S. Katzer, Phys. Rev. B **59**, 8105 (1999).
[8] J. C. Caylor, K. Coonley, J. Stuart, T. Colpitts, and R. Venkatasubramanian, Appl. Phys. Lett. **87**, 023105 (2005).
[9] G. Chen, Phys. Rev. B **57**, 14958 (1998).
[10] G. Chen, J. Heat Transfer **124**, 320 (2002).
[11] M. N. Luckyanova, J. Garg, K. Esfarjani, A. Jandl, M. T. Bulsara, A. J. Schmidt, A. J. Minnich, S. Chen, M. S. Dresselhaus, Z. F. Ren, E. A. Fitzgerald, and G. Chen, Science **338**, 936 (2012).
[12] J. Ravichandran, A. K. Yadav, R. Cheaito, P. B. Rossen, A. Soukiassian, S. J. Suresha, J. C. Duda, B. M. Foley, C.-H. L. Ye Zhu, A. W. Lichtenberger, J. E. Moore, D. A. Muller, D. G. Schlom, P. E. Hopkins, A. Majumdar, R. Ramesh, and M. A. Zurbuchen, Nat. Mater. **13**, 168 (2013).
[13] G. Chen and M. Neagu, Appl. Phys. Lett. **71**, 2761 (1997).
[14] S. Y. Ren and J. D. Dow, Phys. Rev. B **25**, 3750 (1982).
[15] P. Hyldgaard and G. D. Mahan, Phys. Rev. B **56**, 10754 (1997).
[16] D. A. Broido and T. L. Reinecke, Phys. Rev. B **70**, 081310 (2004).
[17] B. Yang and G. Chen, Phys. Rev. B **67**, 195311 (2003).
[18] M. V. Simkin and G. D. Mahan, Phys. Rev. Lett. **84**, 927 (2000).
[19] J. Garg, N. Bonini, and N. Marzari, Nano Letters **11**, 5135 (2011).
[20] J. Garg and G. Chen, Phys. Rev. B **87**, 140302 (2013).
[21] E. S. Landry and A. J. H. McGaughey, Phys. Rev. B **79**, 075316 (2009).
[22] S. Volz, J. B. Saulnier, G. Chen, and P. Beauchamp, High Temp. High Press. **32**, 709 (2000).
[23] W. Zhang, T. Fisher, and N. Mingo, J. Heat Transfer **129**, 483 (2007).
[24] X. B. Li and R. G. Yang, Phys. Rev. B **86**, 054305 (2012).
[25] Z. T. Tian, K. Esfarjani, and G. Chen, Phys. Rev. B **86**, 235304 (2012).
[26] H. Zhao and J. Freund, J. Appl. Phys. **105**, 013515 (2009).
[27] N. Mingo and L. Yang, Phys. Rev. B **68**, 245406 (2003).
[28] R. Landauer, Philos. Mag. **21**, 863 (1970).
[29] P. E. Hopkins and J. R. Serrano, Phys. Rev. B **80**, 201408 (2009).
[30] L. Hu, L. F. Zhang, M. Hu, J. S. Wang, B. W. Li, and P. Keblinski, Phys. Rev. B **81**, 235427 (2010).
[31] Z. T. Tian, B. E. White, and Y. Sun, Appl. Phys. Lett. **96**, 263113 (2010).
[32] P. X. Chen, N. A. Katcho, J. P. Feser, W. Li, M. Glaser, O. G. Schmidt, D. G. Cahill, N. Mingo, and A. Rastelli, Phys. Rev. Lett. **111**, 115901 (2013).
[33] R. Cheaito, J. C. Duda, T. E. Beechem, K. Hattar, J. F. Ihlefeld, D. L. Medlin, M. A. Rodriguez, M. J. Campion, E. S. Piekos, and P. E. Hopkins, Phys. Rev. Lett. **109**, 195901 (2012).